THE JOURNAL OF BIOLOGICAL CHEMISTRY VOL. 287, NO. 24, pp. 20576–20589, June 8, 2012

Urokinase-type Plasminogen Activator Receptor (uPAR)-mediated Regulation of WNT/β-Catenin Signaling Is Enhanced in Irradiated Medulloblastoma Cells*[S]

Received for publication, February 1, 2012, and in revised form, April 13, 2012 Published, JBC Papers in Press, April 16, 2012, DOI 10.1074/jbc.M112.348888

Swapna Asuthkar[‡], Christopher S. Gondi[‡], Arun Kumar Nalla[‡], Kiran Kumar Velpula[‡], Bharathi Gorantla[‡], and Jasti S. Rao[‡§1]

From the Departments of [‡]Cancer Biology and Pharmacology and [§]Neurosurgery, University of Illinois College of Medicine at Peoria, Peoria, Illinois 61605

Background: uPAR is a multifunctional protein, overexpressed in all human cancers.
Results: uPAR overexpression with radiation enhances β-catenin stabilization, β-catenin gene transcription, and WNT-7a-β-catenin-TCF/LEF-mediated transactivation.
Conclusion: Association of uPAR with β-catenin and various transcription factors involved in embryonic development suggests that uPAR is a potent activator of cancer stemness.
Significance: Targeting uPAR in cancer patients undergoing radiotherapy will have favorable therapeutic implications.

Urokinase plasminogen activator receptor (uPAR) is known to promote invasion, migration, and metastasis in cancer cells. In this report, we showed that ionizing radiation (IR)-induced uPAR has a role in WNT-β-catenin signaling and mediates induction of cancer stem cell (CSC)-like properties in medulloblastoma cell lines UW228 and D283. We observed that IR induced the expression of uPAR and CSC markers, such as Musashi-1 and CD44, and activated WNT-7a-β-catenin signaling molecules. Overexpression of uPAR alone or with IR treatment led to increased WNT-7a-β-catenin-TCF/LEF-mediated transactivation, thereby promoting cancer stemness. In contrast, treatment with shRNA specific for uPAR (pU) suppressed WNT-7a-β-catenin-TCF/LEF-mediated transactivation both *in vitro* and *in vivo*. Quercetin, a potent WNT/β-catenin inhibitor, suppressed uPAR and uPAR-mediated WNT/β-catenin activation, and furthermore, addition of recombinant human WNT-7a protein induced uPAR, indicating the existence of a mutual regulatory relationship between uPAR and WNT/β-catenin signaling. We showed that uPAR was physically associated with the WNT effector molecule β-catenin on the membrane, cytoplasm, and nucleus of IR-treated cells and CSC. Most interestingly, we demonstrated for the first time that localization of uPAR in the nucleus was associated with transcription factors (TF) and their specific response elements. We observed from uPAR-ChIP, TF protein, and protein/DNA array analyses that uPAR associates with activating enhancer-binding protein 2α (AP2a) and mediates β-catenin gene transcription. Moreover, association of uPAR with the β-catenin·TCF/LEF complex and various other TF involved during embryonic development and cancer indicates that uPAR is a potent activator of stemness, and targeting of uPAR in combination with radiation has significant therapeutic implications.

Medulloblastoma accounts for 15% of all brain tumors in children (1). Treatment of medulloblastoma includes surgery, radiation therapy, and chemotherapy. Despite improved radiation therapy techniques, 50% of medulloblastomas are known to recur (1, 2). Reduced radiation dose in combination with molecular targeted therapy is now being studied as an alternative to traditional approaches.

Urokinase-type plasminogen activator (uPAR)[2] is overexpressed in the tumor-stromal invasive microenvironment in many human cancers (3, 4). The role of uPAR in tumor progression and angiogenesis is well characterized (5–7). Targeting uPAR has shown a promising anti-tumor effect in treatment of uPAR-overexpressing tumors (8, 9). Most recently, uPAR has been shown to be overexpressed after IR treatment, and its suppression caused reduced invasion and migration in medulloblastoma cells (10). uPAR overexpression in human breast cancer cells was shown to promote cancer stem cell (CSC)-like properties, which include increased expression of CD44, β1/CD29, and α6/CD49f molecules (11). Thus relevance of uPAR at facilitating the development of CSC is very evident and needs to be studied further.

Medulloblastomas, also known as primitive neuroectodermal tumors, have aberrant activation of developmental signaling pathways such as WNT, SHH, and NOTCH (12, 13). Activation of the WNT signaling pathway has been reported in 25% of sporadic medulloblastomas, and these include 15% of cases with mutations in *CTNNB1* (encoding β-catenin), *APC*, and *AXIN1* (14). This study on medulloblastoma stem cells links overexpression of uPAR with activation of WNT/β-catenin sig-

* This work was supported, in whole or in part, by National Institutes of Health Grant CA138409 (to J. S. R.).
[S] This article contains supplemental Figs. 1–3, Tables 1–4, and Materials and Methods.
[1] To whom correspondence should be addressed: Dept. of Cancer Biology and Pharmacology, University of Illinois College of Medicine, One Illini Dr., Peoria, IL 61605. Tel.: 309-671-3445; E-mail: jsrao@uic.edu.

[2] The abbreviations used are: uPAR, urokinase plasminogen activator receptor; IR, ionizing radiation; CSC, cancer stem cell; TF, transcription factor; IP, immunoprecipitation; NE, nuclear extract; ME, membrane extract; CF, culture filtrate; ruPAR, recombinant uPAR; Fl-uPAR, full-length uPAR.

naling, which is enhanced upon radiation treatment. Canonical WNT signaling pathway is a critical regulator of stem cell signaling through key molecules such as the β-catenin and T-cell factor/lymphoid enhancer factor (TCF/LEF) family of transcription factors (15). This β-catenin·TCF/LEF complex in the nucleus is known to increase transcription of proto-oncogenes such as c-*myc*, MMPs, c-*jun*, *fra-1,* and uPAR (16), thereby indicating that a possible cross-talk exists between uPAR and the β-catenin signaling pathway.

Jankun *et al.* (17) showed localization of uPAR on the cell surface and in the nucleus of breast cancer cells. Later, Dumler *et al.* (18) demonstrated co-internalization of the uPAR·nucleolin complex inside the cell, which emphasizes the possibility of nuclear translocation of uPAR. We show that IR-induced overexpression of uPAR leads to uPAR translocation in the nucleus and its association with different transcription factors that may facilitate maintenance of stemness. Furthermore, our studies explored the role of uPAR and its association with WNT/β-catenin signaling in medulloblastoma stem cells upon IR treatment.

EXPERIMENTAL PROCEDURES

Cell Lines, CSC Neurospheres, Spheroids, Transfection, and Radiation—The early passage culture of human medulloblastoma cell lines UW228 (a kind gift from Dr. Francis Ali-Osman) and D283 Med (ATCC HTB 185) were maintained in RPMI and Advanced-MEM, respectively (19). CSC neurospheres were obtained from parental UW228 and D283 cells as described previously (20). Primary neurospheres were obtained in 5–6 days and were subsequently disturbed by trituration; single cell suspension obtained was then plated for secondary neurosphere formation. Neurospheres around 8–14 passages were used for this study. Neurospheres were examined for CSC-like properties by neurosphere formation assay. In a separate experiment, spheroids were formed as described previously (21). For combination treatments, a radiation dose of 6 gray was given using RS 2000 Biological Irradiator x-ray unit (Rad Source Technologies Inc., Boca Raton, FL) (see supplemental Methods).

Plasmids, shRNA Constructs, Antibodies, Inhibitors, and Reagents—We used uPAR human cDNA cloned in pCMV6-AC vector (Origene, Rockville, MD) for full-length uPAR (Fl-uPAR) overexpression, and uPAR-overexpressing stable cells in our study are considered as Fl-uPAR cells. Vector alone was used as a control. Monocistronic pU and bicistronic pUM constructs designed to knock down uPAR and MMP-9 were generated in our laboratory (22). A pCDNA3-scrambled vector with an imperfect sequence (pSV) was used as a control. HSP90β (h) siRNA was purchased from Santa Cruz Biotechnology (Santa Cruz, CA). A cignal TCF/LEF reporter (luc) construct (CCS-018L) encoding firefly luciferase reporter gene along with a constitutively expressing *Renilla* luciferase construct (40:1) (SABiosciences, Frederick, MD) were used to monitor WNT signaling activity. Appropriate positive and negative control reporter plasmids were used, and all transfections were normalized to *Renilla* luciferase activity. Quantification of both firefly and *Renilla* luciferase reporters were done by using Dual-Luciferase® Reporter (DLR™) assay system (Promega, Madison, WI). Relative luciferase units were measured in a luminometer (TD-20/20 DLReady) for cell suspension/*In Vivo* Imaging System (Xenogen, Alameda, CA) for spheroids. The following antibodies were used: anti-uPAR, β-catenin, TCF-1, LEF-1, WNT-7a, STRO-1, MSI-1, CD44, pGSK3β (Ser-9), HSP90β, CD133, and AP-2a were purchased from Santa Cruz Biotechnology; p-β catenin (Ser-33/37/Thr-41) was purchased from Cell Signaling (Beverly, MA), and WNT-1 was purchased from Abcam (Cambridge, MA). Recombinant human WNT-7a protein was purchased from R & D systems (Minneapolis, MN), and AP2α protein was purchased from Novus Biologicals (Littleton, CO). Quercetin (100 μM) was purchased from Sigma.

Establishment of Stable Cells Expressing TCF/LEF GFP Constructs—D283 cells were transduced at 80% confluence in 6-well culture plates with Cignal Lenti TCF/LEF Reporter (GFP) construct with VSV-g pseudotyped lentivirus particles expressing a GFP gene under a minimal CMV promoter and tandem repeats of TCF/LEF according to manufacturer's guidelines (SA Biosciences). The medium was replaced with normal growth medium and incubated for 48 h. On day 3, cells were selected in 10 μg/ml puromycin containing medium. Around 13 puromycin-resistant single cell colonies were obtained with cloning rings and expanded. The clone with the highest GFP expression was further maintained in the medium containing 2.5 μg/ml puromycin and was used for this study. D283-TCF/LEF GFP stable cells were used to form self-renewing, free-floating neurospheres and were passaged every 8th day in 60-mm plates.

Subcellular Protein Fractionation, Western Blotting, Immunoprecipitation, and Mass Spectrometry—Nuclear extracts and Triton X-114-mediated phase partitioning was performed according to standard protocol (19). Immunoprecipitation (IP) assays were carried out by incubating 400 μg of nuclear/membrane/cytoplasmic extracts with specific primary antibody (2 μg) overnight at 4 °C on an end-to-end rotator. Next, Catch and Release Version 2.0 IP kit (Millipore, Temecula CA) was used to immunoprecipitate and elute proteins in denaturing or nondenaturing buffers according to the manufacturer's instructions. Immunoprecipitates were immunoblotted using specific primary antibodies. LC-MS/MS spectra analysis of immunoprecipitated membrane extract proteins of UW228 and D283 using anti-uPAR antibody was generated following standard protocol (see supplemental Methods) (23) (University of Florida), and obtained sequences were compared using NCBI Blastp tool.

Immunoflow Cytometry, Immunocytochemistry, and Immunohistochemistry—Flow cytometric immunofluorescence assay was done to demonstrate expression levels of uPAR and MSI-1 in control, Fl-uPAR, and CSCs alone and with IR treatment. (see supplemental Methods).

Chromatin Immunoprecipitation (ChIP), Cloning, DNA Sequencing, and TF-binding Site Prediction—ChIP assay was performed using ChIP-IT™ Express kit from Active Motif (Carlsbad, CA) following supplied protocol (see supplemental Methods).

Real Time PCR Analysis—The WNT signaling specific primers are listed insupplemental Table 1. mRNA transcript levels of WNT signaling molecules were examined by real time PCR

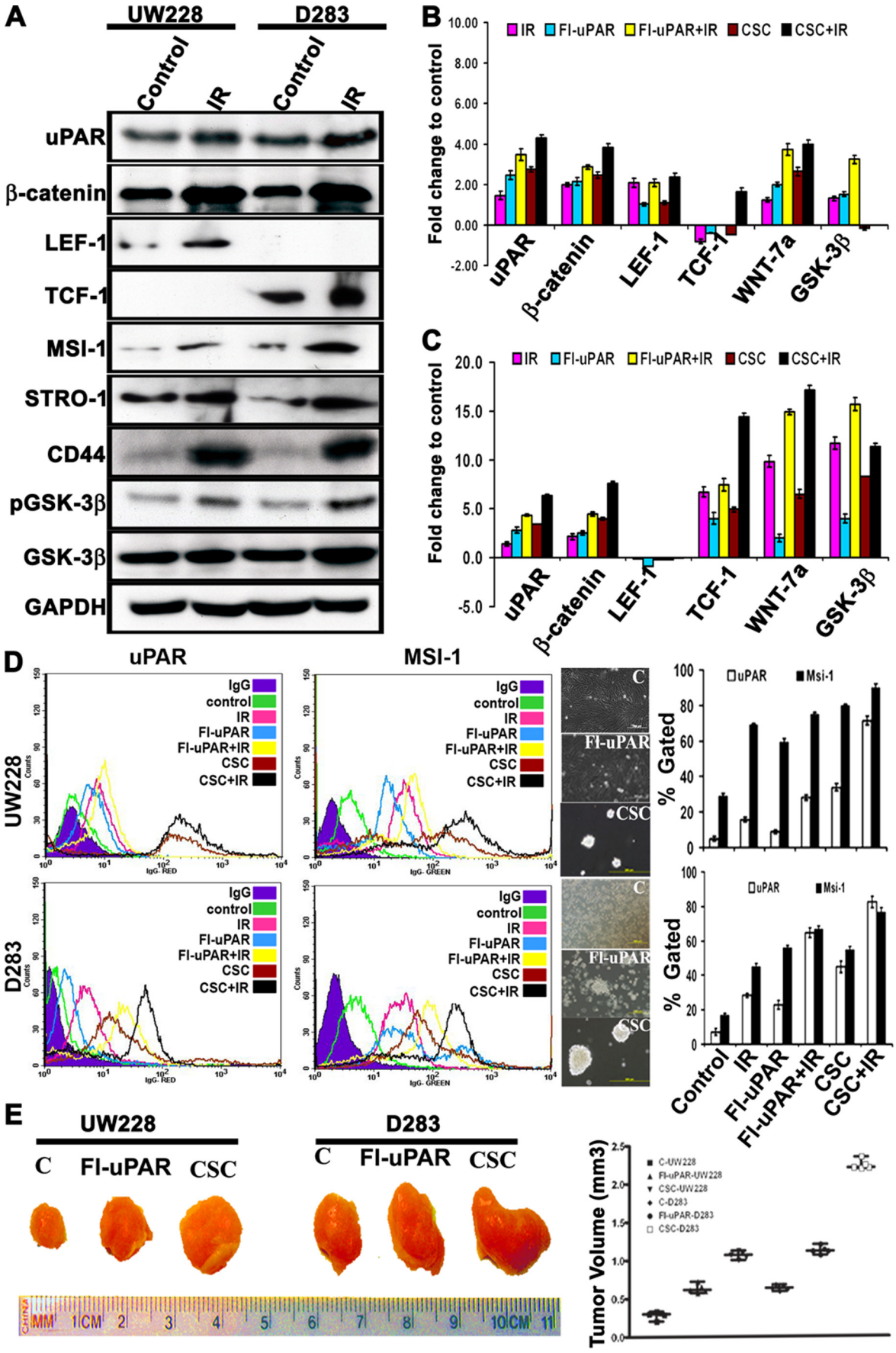
A
UW228
D283
Control
IR
Control
IR
uPAR
β-catenin
LEF-1
TCF-1
MSI-1
STRO-1
CD44
pGSK-3β
GSK-3β
GAPDH
B
IR
Fl-uPAR
Fl-uPAR+IR
CSC
CSC+IR
Fold change to control
uPAR
β-catenin
LEF-1
TCF-1
WNT-7a
GSK-3β
C
D
uPAR
MSI-1
UW228
D283
IgG
control
IR
Fl-uPAR
Fl-uPAR+IR
CSC
CSC+IR
C
Fl-uPAR
CSC
% Gated
Control
E
UW228
D283
C
Fl-uPAR
CSC
Tumor Volume (mm3)
C-UW228
Fl-uPAR-UW228
CSC-UW228
C-D283
Fl-uPAR-D283
CSC-D283

using CFX96™ real time system (Bio-Rad) (see supplemental Methods).

TF, TF·DNA Interaction Arrays, and EMSA—TranSignal™ TF protein arrays version I, II, and IV (Panomics, Fremont, CA) were used to study protein/protein interactions between human recombinant uPAR (ruPAR) (R&D Systems, Inc., MN) protein (bait) with multiple transcriptional factors (TF) immobilized on membranes. Protein array membranes (MA3501, MA3502, and MA3504) were blocked and incubated with 3 μg of ruPAR protein overnight at 4 °C with gentle shaking. Membranes were washed and incubated with anti-uPAR antibody for 2 h and subsequently with secondary antibody for 1 h at RT. The spots were detected using chemiluminescence detection buffer. In a separate experiment, interaction of uPAR with TF-binding oligonucleotide probes was shown using protein·DNA array version I (Panomics). Nuclear extracts from Fl-uPAR-transfected and IR-treated D283 cells were subjected to IP using anti-uPAR antibody and were eluted in nondenatured form. Eluted fraction (3 μg) was incubated with biotin-labeled DNA-binding probes for 56 TFs (MA1210) to form protein·DNA complexes. Probes in the complexes were then extracted and hybridized to protein·DNA array I and detected using HRP-based chemiluminescence detection buffer by following manufacturer's protocol. Binding of uPAR to TFs was observed as spots on x-ray film. TCF/LEF and AP-2(1) electrophoretic mobility shift assays (EMSA) using 2 μg of nuclear extract was performed according to manufacturer's instructions (Panomics).

Subcutaneous Tumor (s.c.) Growth—We carried out s.c. implantation as described previously (24). Tumor volume was calculated from formula 1/6 II $(R_{max}) \times (R_{min})^2$, where R_{max} and R_{min} are maximum and minimum tumor radii, respectively.

Surgical Orthotopic Implantation of D283 TCF/LEF-GFP Stable Cell Neurospheres—Athymic nude mice at about 3 weeks of age were used for intracerebral injections. Mice were anesthetized using isoflurane gas anesthesia (~2%) and placed into a stereotaxic frame (David Kopf Instruments, Tujunga, CA). A drill hole (0.5 mm diameter) was created through the skull, and D283 TCF/LEF-GFP neurospheres (1×10^5 cells/10 μl of PBS), with or without IR treatment, were implanted into the brain at a depth of 3 mm. Twelve days after tumor cell implantation, animals were randomized into four treatment groups as pSV, pSV + IR, pU, and pU + IR ($n = 5$). Each animal was treated intravenously with either pU or pSV (6–8 mg/kg body weight) plasmids on the 12th and 16th day. Animals that lost ≥20% of body weight or had trouble ambulating or feeding were sacrificed. Animals were monitored for 45 days, which is when the experiment was terminated. Mouse brains were subjected to GFP imaging by stereo zoom dissection microscope (SZX12, Olympus, Melville, NY), before they were fixed in 10% buffered formalin and processed for paraffin embedding. Tissue sections (5 μm thick) were obtained from paraffin blocks and stained with H&E using standard histological techniques.

Statistical Analysis—All data are presented as means ± S.E. of at least three independent experiments. One-way analysis of variance combined with Tukey post hoc test of means were used for multiple comparisons. Statistical differences are presented at $p < 0.05$, $p < 0.01$, and $p < 0.001$.

RESULTS

IR Induces uPAR Overexpression and Activation of WNT/β-Catenin Signaling—We have previously described that IR treatment increases uPAR expression and activates uPAR-dependent cell signaling (10). Furthermore, IR has been shown to induce radioresistance by aberrant activation of key stem cell pathways such as WNT/β-catenin (25). Our Western blot results showed up-regulation of uPAR, cancer stem cell (CSC) markers, including CD44, MSI-1, STRO-1, and WNT signaling molecules such as β-catenin and LEF/TCF-1 in IR-treated cells ($p < 0.001$), when compared with control UW228 and D283 cells. Interestingly, we observed LEF-1 in UW228 cells and TCF-1 in D283 cells. Furthermore, IR treatment showed increased inactivation of GSK3β by phosphorylation at Ser-9 position ($p < 0.01$) (Fig. 1*A*). Inactivation of GSK3β leads to β-catenin stabilization and activation of β-catenin·TCF/LEF signaling (26). To determine whether IR-induced uPAR has a role in transcriptional activation of WNT/β-catenin signaling necessary for CSC, we performed real time PCR in control, Fl-uPAR, CSCs alone, and in combination with IR treatments. We observed that increased uPAR levels with IR treatment showed synergistic increase in mRNA transcript levels of β-catenin, TCF/LEF-1, and WNT-7a in both UW228 and D283 cells ($p < 0.05$). CSCs with IR treatment showed a prominent increase in expression levels of uPAR and WNT molecules (Fig. 1, *B* and *C*). We also observed a significant increase in mRNA transcript levels of GSK3β; however, protein levels of GSK3β in the immunoblot showed only a slight increase in IR-treated cells when compared with control cells.

We used immuno-flow cytometry to examine whether uPAR overexpression with IR altered the abundance of MSI-1, whose expression is known to be regulated by the WNT pathway (27). The levels of uPAR and MSI-1 were substantially increased in IR-treated UW228 and D283 cells and CSCs. uPAR overexpressing (Fl-uPAR) cells also showed increased levels of MSI-1 (Fig. 1*D*). Moreover, both UW228 and D283 cells formed neurospheres with self-renewal capacity, and we observed that the neurosphere-forming ability of medulloblastoma cells was enhanced after IR treatment (supplemental Fig. 1). Furthermore, we verified the ability of IR-treated control cells, Fl-uPAR cells, and CSCs to form tumors by a subcutaneous tumor model

FIGURE 1. **IR treatment induces the abundance of uPAR and CSC markers.** *A,* Western blot analysis of cell lysates (40 μg) from control and IR-treated UW228 and D283 cells. The blots were developed using antibodies specific for uPAR, β-catenin, LEF-1, TCF-1, MSI-1, STRO-1, CD44, pGSK3β (Ser-9), and GSK3β; GAPDH was used as a loading control. *B* and *C,* real time PCR analysis of the control, Fl-uPAR cells, and CSCs alone and in combination with IR treatment in UW228 (*B*) and D283 cells (*C*). Transcript levels of uPAR, β-catenin, LEF-1, TCF-1, WNT-7a, and GSK3β were analyzed in the treated cells and represented graphically as the fold change expression compared with the control cells. GAPDH was used as the internal control. The *bar graphs* are the means± S.D. from three independent experiments ($p < 0.05$). *D,* immunoflow cytometry to detect uPAR and MSI-1 in control (*green*), Fl-uPAR (*red*), and CSCs (*blue*) alone and in combination with IR-treated UW228 and D283 cells. The isotype-matched IgG (*purple*) was used as negative control. *E,* tumor forming ability of IR-treated UW228 and D283 control, and Fl-uPAR and CSC were verified by subcutaneous tumor model studies. Semiquantification of tumor volume in treated groups was done as described under "Experimental Procedures," and the data shown are the means ± S.D. values from five animals from each group ($p < 0.001$).

assay. We observed that the subcutaneous tumor-forming ability of Fl-uPAR cells and CSC ($p < 0.01$) was more when compared with control cancer cells. Interestingly, we also observed that subcutaneous tumors formed by IR-treated D283 cells showed increased tumor volume when compared with UW228 cells ($p < 0.001$) (Fig. 1*E*).

Mutual Regulation between uPAR and β-Catenin·TCF/LEF Molecules with IR Treatment—Fl-uPAR-transfected cells with IR treatment showed increased levels of β-catenin, LEF/TCF-1, pGSK3β, and MSI-1 by 34, 59, 24, and 29%, respectively and decreased levels of p-β-catenin by 36% when compared with IR-treated control cells. Interestingly, we also observed increased WNT-7a protein expression in culture filtrates (CF) of Fl-uPAR and IR-treated cells. Moreover, addition of quercetin to these cells suppressed uPAR and uPAR-mediated increase in canonical WNT signaling molecules ($p < 0.01$) (Fig. 2, *A* and *B*). Furthermore, activation of WNT/β-catenin signaling is known to increase transcription of uPAR and involves transcriptional activation of β-catenin (28) Thus, it is apparent that mutual regulatory mechanisms exist between uPAR and β-catenin signaling. In medulloblastoma cells, we found that addition of increasing concentrations of WNT-7a protein (0, 50, 100, and 200 ng/ml) induced β-catenin levels in whole cell lysates and nuclear extracts (supplemental Fig. 1*C*) and also enhanced the β-catenin·TCF/LEF-mediated reporter activity (supplemental Fig. 1*D*) in a dose-dependent manner. WNT-7a protein at 200 ng of concentration showed around 70% increase in nuclear translocation of β-catenin. Furthermore, we observed that addition of WNT-7a (200 ng/ml) alone or in combination with radiation showed increased β-catenin and uPAR expression ($p < 0.01$) (Fig. 2*C*). The p-β-catenin levels were decreased in WNT-7a-treated cells. WNT-7a immunoblot results of UW228 and D283 cells were similar to Fl-uPAR results as shown in Fig. 2, *A* and *B*, which showed that both uPAR and WNT-7a can mutually up-regulate each other's expression.

uPAR Is Associated with WNT/β-Catenin Signaling—Because uPAR is one of the transcriptional targets of β-catenin·TCF/LEF signaling (29), we performed immunocytochemistry analysis in cancer cells and CSCs to study their association (Fig. 3*A* and supplemental Fig. 2*C*). We observed that levels of uPAR and β-catenin were abundant in the membrane, cytoplasm, and nucleus of IR-treated cells and CSCs, when compared with controls. Interestingly, in control cells, we observed co-localization of uPAR with β-catenin on membrane (Fig. 3*A, lanes 1* and *3*), whereas in IR-treated cells we observed increased association of uPAR and β-catenin, which was more prominent in the nucleus (Fig. 3*A, lanes 2* and *4*). To confirm the above results, we performed IP studies using cellular extracts of UW228 and D283 control and IR-treated cells. The IP of nuclear extracts (NE) using anti-uPAR and reverse pull-down IP using anti-β-catenin antibody confirmed the association between uPAR and β-catenin in NE (Fig. 3*B* and supplemental Fig. 2*A*). From IP of membrane extracts (ME), we also confirmed the association of uPAR and β-catenin in ME (Fig. 3*B*). Consistent with these results, uPAR was found to be co-localized with β-catenin in human medulloblastoma tumor tissue array (US Biomax, Rockville, MD) (Fig. 3*D*).

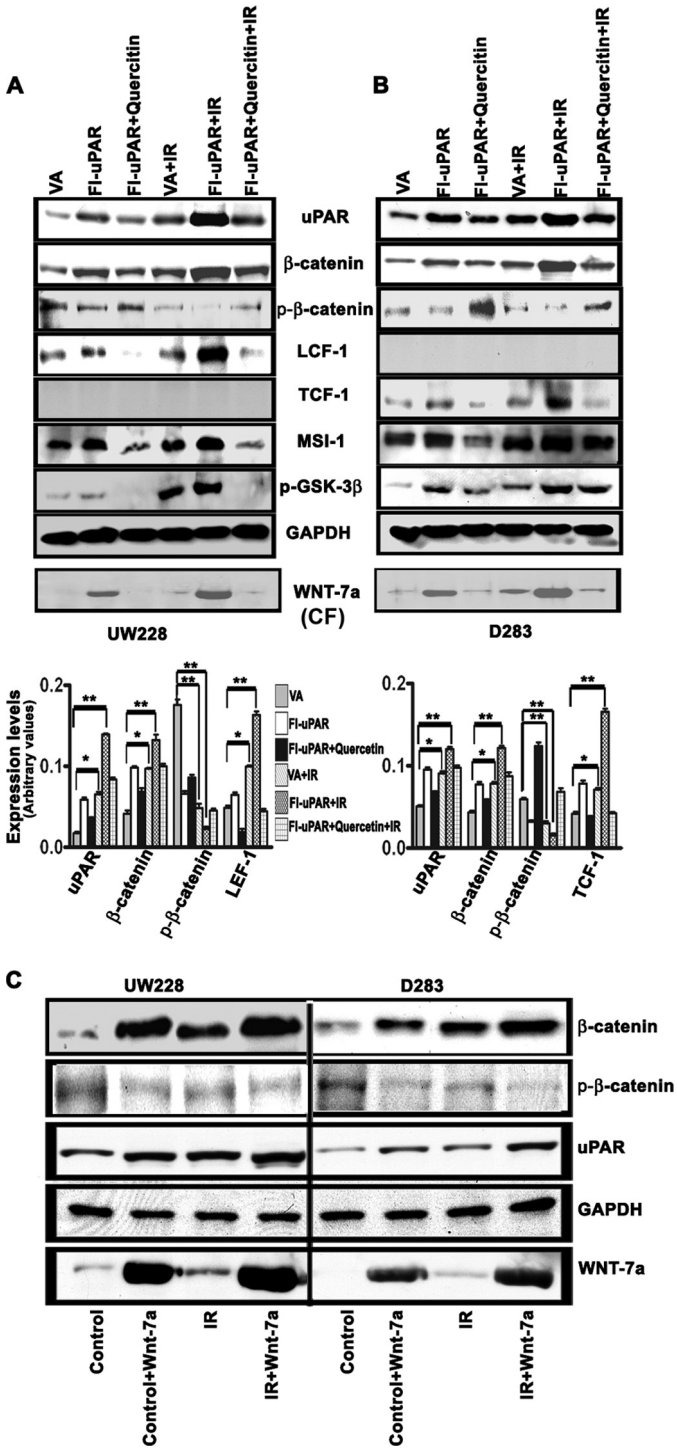

FIGURE 2. **Mutual regulation of uPAR overexpression and β-catenin·TCF/LEF signaling with IR treatment.** The immunoblot analysis of WNT/β-catenin signaling of downstream molecules in whole cell lysates of UW228 (*A*) and D283 (*B*) cells treated with vector alone (*VA*), full-length uPAR-overexpressing plasmid and Fl-uPAR + 100 μM quercetin alone and in combination with IR treatment. GAPDH was used as the loading control. Quantitative analysis was done by optical densitometry and represented graphically as means ± S.D. from three independent experiments (*, $p < 0.01$; **, $p < 0.001$). *C*, immunoblot analysis of whole cell lysates from UW228 and D283 cells treated with recombinant human WNT-7a protein alone and in combination with IR treatment. The blots were developed using antibodies specific for β-catenin, p-β-catenin, and uPAR; GAPDH was used as the loading control. The WNT-7a protein was analyzed in CF by immunoblot.

Furthermore, immunoblots from IP studies were re-probed using anti-LEF/TCF antibodies, which detected that LEF/TCF proteins were co-precipitated with uPAR in NE but not in ME (Fig. 3*B*). Furthermore, to examine the role of uPAR in β-catenin·TCF/LEF-mediated transactivation activity, we performed EMSA. We observed that IR treatment up-regulated β-catenin·TCF/LEF activity in UW228 and D283 cells. Incubation of IR-treated NE with anti-uPAR antibody induced a supershift in the LEF/TCF-·DNA complex migration; however, we observed that not all the LEF/TCF was bound to uPAR (Fig. 3*C* and supplemental Fig. 2*B*).

Moreover, mass spectrometry analysis of a prominent 90-kDa protein band (corresponding to molecular weight of

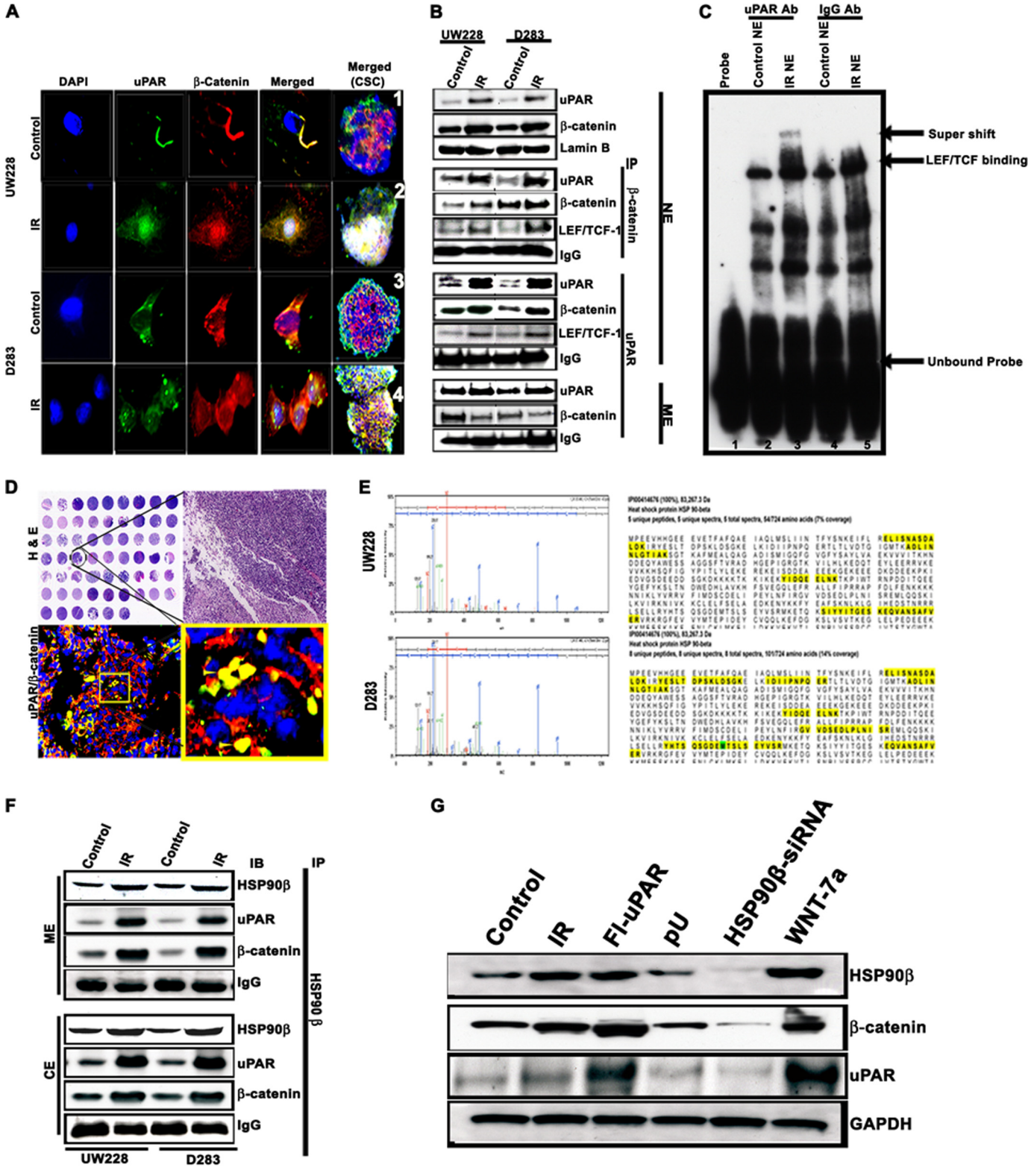

β-catenin) obtained by immunoprecipitating uPAR from ME of control and IR-treated UW228 and D283 cells identified heat-shock protein 90β (HSP90β) (Fig. 3*E*). Because uPAR is devoid of the transmembrane and cytoplasmic domain, we anticipated that association of uPAR with β-catenin would involve other interlinking molecules. Accordingly, our study further examined if HSP90β acted as an interlinking molecule between uPAR and β-catenin. Our subsequent IP of membrane and whole cell extracts using anti-HSP90β antibody indicated association of uPAR·β-catenin·HSP90β, which was noticeably enhanced after IR treatment (Fig. 3*F*). Furthermore, we examined HSP90β, uPAR, and β-catenin expression levels in control, IR, Fl-uPAR, pU, HSP90β-siRNA, and WNT-7a-treated cells. We found that following IR, uPAR, and WNT-7a overexpression treatments, increased expression of HSP90β protein and up-regulated uPAR and β-catenin levels were shown. Conversely, pU and HSP90β-siRNA treatments showed down-regulation of these proteins (Fig. 3*G*).

uPAR Knockdown Suppressed Canonical WNT Pathway in Vitro—Western blot analyses of IR-treated UW228 and D283 CSCs showed increased levels of β-catenin in nuclear extracts (NE), uPAR, CD133 in cytoplasmic extracts (CE), and WNT-7a in culture filtrate (CF), when compared with controls. Because recent studies showed MMP-9 as a key indicator of WNT activation in embryonic neural stem cells (30), we checked the activity of MMP-9 using CF of CSCs. We observed increased MMP-9 activity after IR treatment, which was correlated to WNT-7a expression in CF and β-catenin levels in NE (Fig. 4, *A* and *B*). Furthermore, to replicate a three-dimensional model of an intracranial tumor, we developed spheroids of UW228 and D283 CSCs for our studies. To assess the activity of the WNT pathway, spheroids were transfected with the cignal TCF/LEF reporter (luc) construct encoding firefly luciferase. Using the TCF/LEF reporter assay, we found that the sublethal doses of IR induced WNT pathway activation in both UW228 (Fig. 4*A1*) and D283 (Fig. 4*B1*) CSC spheroids. The 6 gray radiation dose was determined to be appropriate for our studies in medulloblastoma cell lines, as this dose showed increased transactivation of β-catenin-TCF/LEF when compared with controls ($p < 0.01$) (Fig. 4, *A* and *B*).

Additionally, to examine whether uPAR signals through β-catenin, the spheroids were transfected using pU/pUM constructs, designed to knock down uPAR and MMP-9, and also simultaneously with cignal TCF/LEF reporter (luc) construct. The IR treatment increased spheroid migration (Fig. 4, *C* and *D*) and expression of migration-associated molecules such as β-catenin and uPAR as determined by RT-PCR analysis (Fig 4, *C2* and *D2*). The pU and pUM treatments resulted in loose, poorly adherent, and less invasive spheroids and suppressed TCF/LEF reporter activity in IR-treated spheroids (Fig. 4, *C1* and *D1*). The pU and pUM treatment also showed increased p-β-catenin and decreased nuclear translocation of β-catenin·TCF/LEF proteins after IR treatment ($p < 0.05$). Moreover, we observed lower MMP-9 and WNT-7a levels after pU/pUM treatment of CSCs (Fig. 4*E*).

uPAR Knockdown Suppressed in Vivo Canonical WNT Pathway—D283-TCF/LEF GFP stable cells were enriched for CSCs by subjecting to neurosphere formation (Fig. 5*A1*) followed by IR treatment, after which neurosphere suspension was implanted in the cerebellum region of nude mice. IR-treated D283-TCF/LEF GFP stable cell neurospheres showed increased migration to parts of the cerebellar hemisphere. The pU and pU + IR treatment showed lower GFP expression and reduced migration, wherein GFP expression was restricted to the site of injection when compared with the respective controls (Fig. 5*A2*).

Furthermore, IR-treated tumors showed lower tumor burden and scattered tumor presence with multiple tumor foci, when compared with non-IR treated tumors in H&E staining. In contrast, pU- and pU + IR-treated mice failed to form aggressive tumors and showed decreased tumor burden (supplemental Fig. 3*A, lane 1*). We further performed 3,3′-diaminobenzidine staining, which confirmed increased β-catenin and uPAR expression in tumor regions. From 3,3′-diaminobenzidine staining, we observed several brown spots of β-catenin and uPAR within the nucleus, which were more prominent in IR-treated tumors. The pU- and pU + IR-treated tumors showed low levels of β-catenin and its nuclear localization (supplemental Fig. 3*A, lanes 2* and *3*). Additionally, immunofluorescence studies using Alexa Fluor-conjugated secondary antibody against uPAR (Fig. 5*B*, *blue*) and β-catenin (*red*) confirmed their association (*pink*) in *in vivo* tumors. In IR-treated tumors, we observed increased uPAR and β-catenin levels that were spread throughout the tumor region. In both non-IR and IR-treated tumors, suppression of uPAR inhibited β-catenin expression (Fig. 5*B*).

FIGURE 3. **Association of uPAR with β-catenin in the membrane and nucleus of UW228 and D283 cells.** *A,* immunocytochemistry analysis of UW228 and D283 control and IR-treated cells and CSCs grown on chambered slides were immunoprobed for uPAR and β-catenin (1:100), incubated with secondary antibodies, and conjugated with Alexa Fluor green (uPAR) and red (β-catenin) at a concentration of 1:200 as described in supplemental Materials and Methods. Only the merged figures of CSC are represented here, and the individual stained figures are shown in supplemental Fig. 2*C*. *B,* IP was performed using anti-uPAR antibody and reverse pulldown IP using anti-β-catenin antibody to show the association of uPAR with β-catenin·TCF/LEF in the nuclear extract (NE) of control and IR-treated UW228 and D283 cells. The IP using anti-uPAR antibody was performed to show the association of uPAR with β-catenin in the membrane extract (ME) as described under "Experimental Procedures." IgG denotes the anti-IgG antibody control in the IP assays. *C,* EMSA was performed with 2 μg of NE from treated cells. *1st lane* is for the TCF/LEF probe in the absence of NE and antibody; *2nd* and *3rd lanes* show NE of control and IR-treated D283 cells, respectively, in the presence of anti-uPAR antibody (*uPAR Ab*); *4th* and *5th lanes* show NE of control and IR-treated D283 cells, respectively, in the presence of IgG antibody (IgG). *D,* medulloblastoma brain tissue microarray, containing 20 cases of medulloblastoma of brain consisting of 60 cores. Tissue arrays were processed for immunohistochemistry using anti-uPAR (*green*) and anti-β-catenin (*red*) antibodies as described under "Experimental Procedures." Microscopic examination was done (Olympus BX61 Fluoview, Minneapolis, MN) at a ×40 magnification. *E,* LC-MS/MS spectral analysis of a 90-kDa band, immunoprecipitated from the ME of UW228 and D283 control and IR-treated cells using anti-uPAR antibody-identified HSP90β. *F,* IP using anti-HSP90β was performed with ME and whole cell extracts (*CE*) of control and IR-treated UW228 and D283 cells and was immunoblotted (*IB*) against anti-uPAR, β-catenin, and HSP90β. antibodies; IgG denotes the anti-IgG antibody control in the IP assays. *G,* immunoblot analysis of whole cell lysates from control, IR, Fl-uPAR, pU, HSP90β-siRNA, and WNT-7a treated D283 cells. The blots were developed using antibodies specific for HSP90β, β-catenin, and uPAR; GAPDH was used as the loading control.

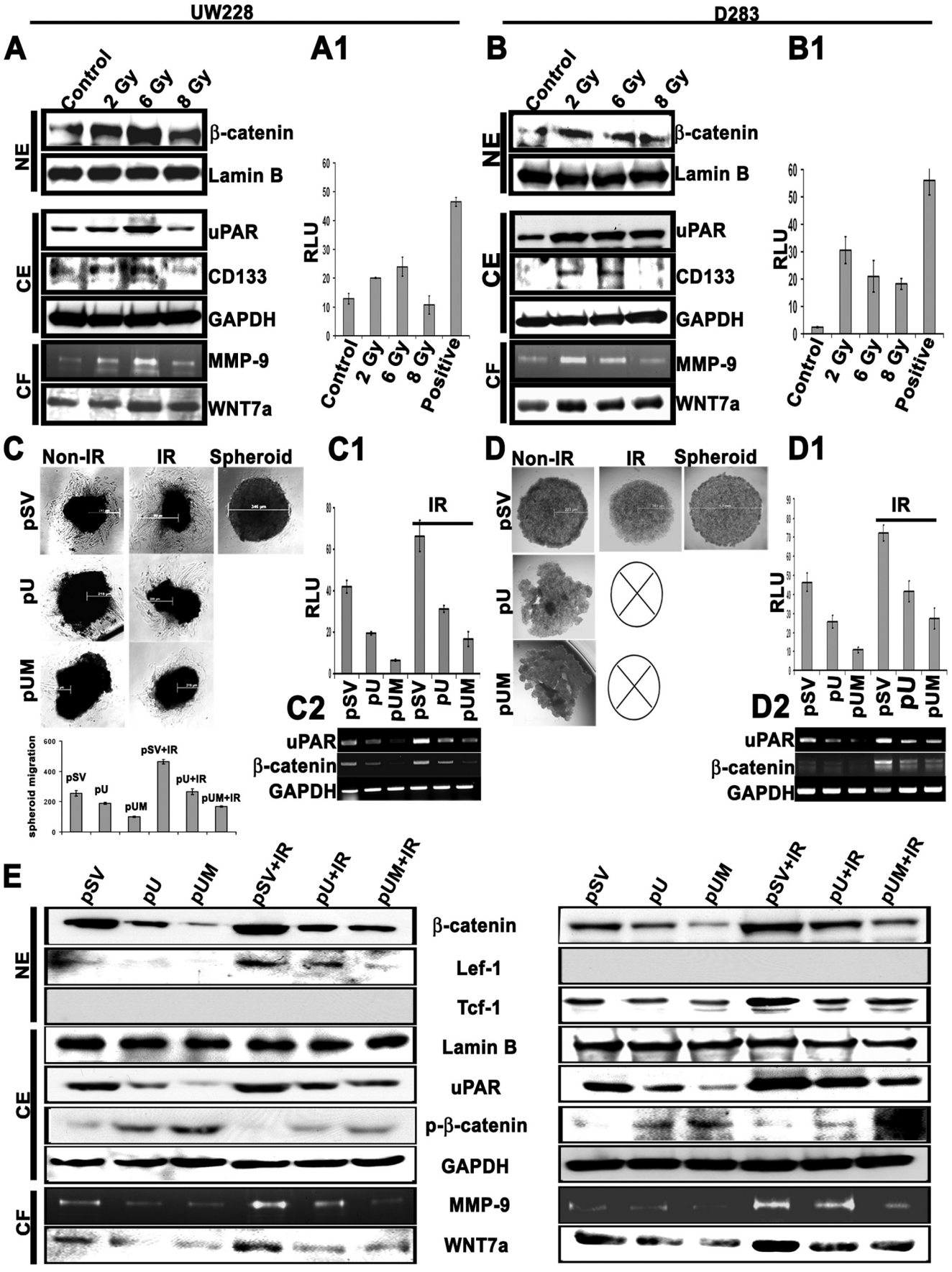
UW228
D283
A
A1
B
B1
Control
2 Gy
6 Gy
8 Gy
NE
CE
CF
β-catenin
Lamin B
uPAR
CD133
GAPDH
MMP-9
WNT7a
RLU
Positive
C
C1
C2
D
D1
D2
Non-IR
IR
Spheroid
pSV
pU
pUM
spheroid migration
pSV+IR
pU+IR
pUM+IR
E
Lef-1
Tcf-1
p-β-catenin

uPAR Association with TF and Role of uPAR in AP-2a-mediated Transcriptional Activation of β-Catenin—uPAR is well known in establishing multiple contacts with various membrane and cytoplasmic proteins (31). Because we observed nuclear localization of uPAR upon IR treatment, we further extended our study to examine the possible association of uPAR with various TF and their response elements. uPAR chromatin immunoprecipitation (ChIP) DNA was isolated from UW228 and D283 control and IR-treated cells that were then cloned, sequenced, and analyzed. ChIP analyses identified a number of short individual sequences, and at least 16 of 29 sequences showed a consensus 48-bp sequence consisting of endogenous AP2a and E2F-1 binding regions (Fig. 6*A*). Furthermore, TranSignal™ TF protein arrays were used to show the protein/protein interactions between human ruPAR, which was used as bait, with multiple TFs immobilized on the membranes. The ruPAR showed binding with various TF (Fig. 6*B* and supplemental Table 2). Next, ruPAR and uPAR immunoprecipitated from nuclear extracts of Fl-uPAR and IR-treated D283 cells were incubated with different TF-binding oligonucleotide probe mixtures, and their interaction was examined using the protein·DNA array. The ruPAR (*green spots*) and nuclear uPAR (*red spots*) interaction results with TF response elements are represented as overlapping *yellow spots* in Fig. 6*C* and are listed in supplemental Table 3. Consistent with ChIP analysis, the TF protein array and protein·DNA array also showed uPAR association with AP2a. Following this, we confirmed the interaction of uPAR with AP2a in control and IR-treated UW228 and D283 cells by immunoprecipitation analysis (Fig. 6*D*). Most interestingly, we observed around 16 putative AP2-binding sites (32) in the promoter region of the human β-catenin gene. A number of these AP2 sites have been shown to play a role in β-catenin expression (33, 34). To investigate whether uPAR binding to β-catenin promoter was localized around these sites, we used UW228 and D283 ChIP DNA immunoprecipitated by anti-uPAR and anti-IgG antibody. ChIP was carried out by scanning the uPAR binding in the first 1.6-kb 5′-flanking region of the human β-catenin gene (EMBL accession number X89448), using semi-quantitative RT-PCR with primers for regions (R) named 1–6. uPAR enrichment at R4 ($p < 0.01$), which includes six putative AP2-binding sites, was greater than at other regions containing AP2 (R3, R5, and R6) or no AP2 (R1 and R2). The coefficient of uPAR interaction to different AP-2 binding regions in the β-catenin promoter indicated that uPAR binds to β-catenin promoter in a region detected by the R4 primers (Fig. 6*E*). To further show the mechanism of this regulation, we treated UW228 and D283 cells with increasing concentrations of AP-2a protein (0, 1, and 5 μg/ml) in combination with IR. Semi-quantitative RT-PCR analysis using cDNA of AP2a-treated cells showed increased mRNA levels of both β-catenin as well as uPAR (Fig. 6*F*). These results confirmed previous studies (33, 35), which showed that both uPAR and β-catenin gene promoters have functional AP2-binding sites. Furthermore, in our studies a sequence of the GAPDH gene (36), not regulated by AP2, was used as internal control. Furthermore, to examine the role of uPAR in AP2-mediated transcriptional activation of β-catenin, we performed AP2 EMSA analysis using NE of control, IR, vector alone, Fl-uPAR, and pU-treated cells. We observed that IR treatment and uPAR overexpression caused an increase in AP2 activity when compared with control and pU-treated cells (Fig. 6*G*). Furthermore, the sequence alignment analysis (supplemental Fig. 3*C*) showed that the AP2 EMSA probe sequence showed significant homology with the putative AP2-binding site on the R4 region of the β-catenin promoter (Fig. 6*E*).

DISCUSSION

The term primitive neuroectodermal tumors has been applied to medulloblastomas to reflect its embryonal nature and for its potential to differentiate into neuronal and glial cells (37). A better understanding of the molecular link between cerebellar development and embryonal brain tumor formation will aid in development of new and novel therapies targeting medulloblastoma. Mutations associated with nuclear translocation of β-catenin show a favorable clinical outcome in treatment of medulloblastomas (14, 38). Earlier, we correlated increased nuclear translocation of β-catenin with increased MMP-9 (matrix metallopeptidase-9) expression and further showed that uPAR was involved in signaling after IR treatment (10, 19). In continuation with our previous study, we demonstrate here that aberrant activation of the canonical WNT signaling pathway in IR-treated medulloblastoma cells is associated with uPAR overexpression. Furthermore, we observed a synergistic increase in the expression of the CSC marker, MSI-1 (musashi-1), in response to uPAR overexpression. MSI-1 expression is known to be regulated by the canonical WNT pathway (27). The literature has shown that both uPAR and MMP-9 are known targets of the β-catenin·TCF/LEF signaling pathway (16, 39). In our studies, we observed that addition of exogenous WNT-7a protein to medulloblastoma cells

FIGURE 4. **uPAR knockdown (pU) suppresses IR-induced WNT signaling in medulloblastoma CSCs.** *A* and *B,* to determine the activation of WNT/β-catenin in control and IR-treated UW228 and D283 CSCs, immunoblot analysis was done with antibodies specific for β-catenin, uPAR, and WNT-7a. Lamin B and GAPDH were used as a loading controls for nuclear extract (NE) and cytoplasmic extract (*CE*), respectively. *A–D,* UW228 and D283 CSCs (3×10^4) were seeded in 96-well plates coated with 1% agarose and cultured on a shaker at 120 rpm for 24 h. After single spheroids formed, the spheroids were given either different doses of IR treatment (*A1* and *B1*) or transfected with pSV/pU/pUM plasmids in combination with IR treatment (*C* and *D*). All the spheroids were simultaneously transfected with a TCF/LEF Reporter (luc) construct as described under "Experimental Procedures." After 16 h, spheroids were transferred to 24-well plates and were allowed to grow for 48 h. The migration distance was measured for UW228 cells. (*A1, B1, C1,* and *D1*) The activity of β-catenin·TCF/LEF signaling was monitored in cultured spheroids using the Dual-Luciferase® reporter (DLR™) assay system, measured by Xenogen IVIS imaging, and represented graphically in terms of relative luciferase units (*RLU*) of firefly/*Renilla* luciferase. Positive in *A1* and *B1* represents the positive control. The positive control denotes the relative luciferase units of the cells that are transfected with a constitutively expressing firefly and *Renilla* luciferase construct. The *error bars* represent mean ± S.D. from three independent experiments ($p < 0.01$). *C2* and *D2,* RNA was isolated from three representative spheroids of each treatment and subjected to RT-PCR analysis using primers specific for uPAR and β-catenin; GAPDH was used as the loading control. *E,* to determine the activation of WNT/β-catenin in pSV-, pU-, and pUM-transfected UW228 and D283 CSCs, immunoblot (*IB*) analysis was done with antibodies specific for β-catenin, LEF-1, TCF-1, uPAR, p-β-catenin, and WNT-7a. Lamin B and GAPDH were used as a loading controls for NE and cytoplasmic extract (*CE*), respectively. Gelatin zymography was performed to determine MMP-9 activity in the CF as described in supplemental Methods. *Gy*, gray.

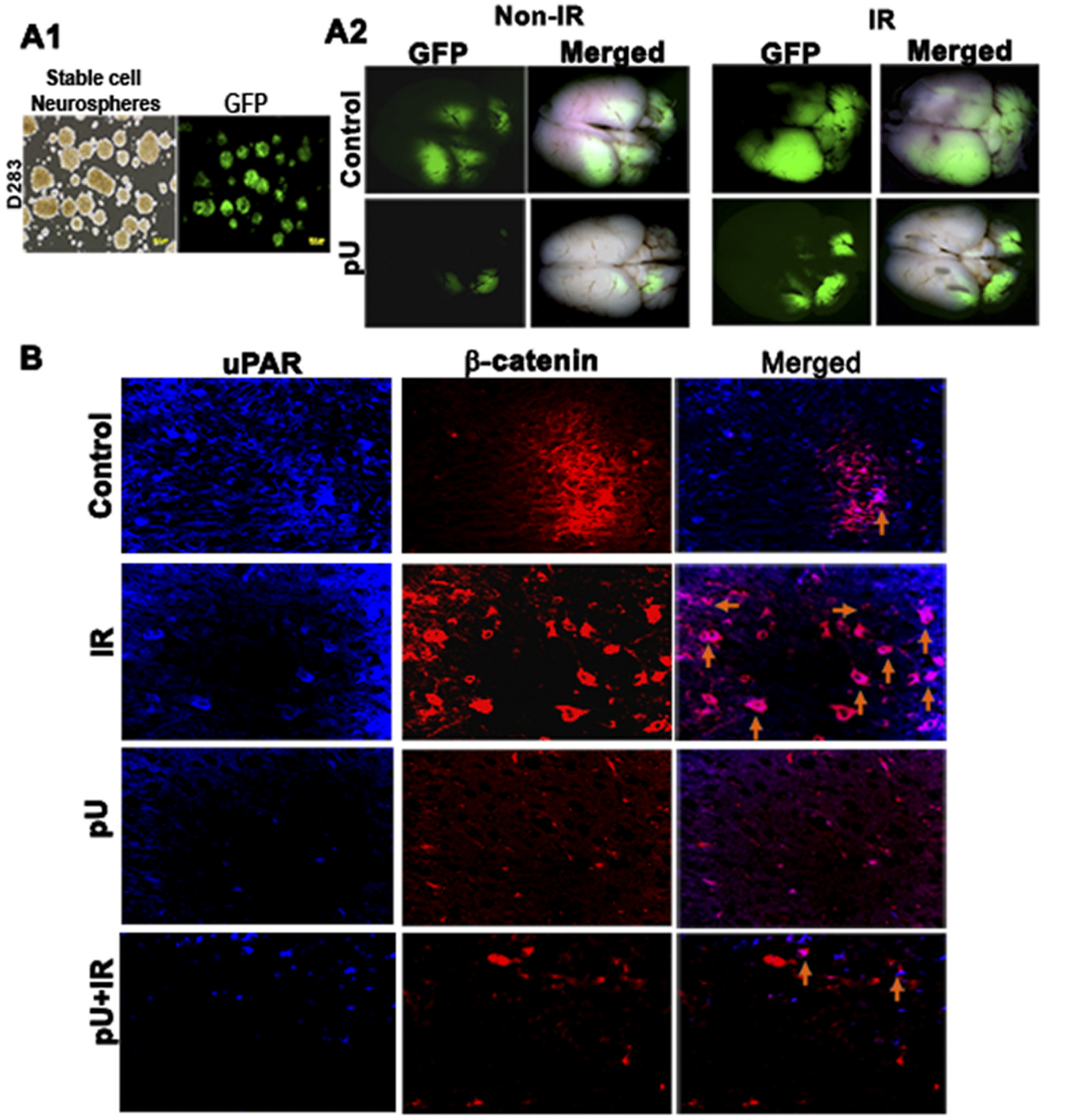

FIGURE 5. **uPAR knockdown (pU) suppresses WNT signaling in *in vivo* tumors.** *A1* and *A2,* intracerebral tumors were established by surgical orthotopic implantation of D283 TCF/LEF-GFP stable cell neurospheres (D283TCF/LEF-GFP neurospheres) in nude mice. The mice were given intravenous treatment of pU plasmids as described under "Experimental Procedures." Mouse brains were subjected to GFP imaging using stereo zoom dissection microscope (SZX12, Olympus, Melville, NY) before fixing in 10% buffered formalin and processed for paraffin embedding. *B,* brain tissue sections were subjected to immunohistochemistry analysis. Immunohistochemical comparison using red and blue Alexa Fluor conjugates for β-catenin and uPAR, respectively.

showed increased uPAR expression. Therefore, to understand the role of these molecules in relation to stemness, we studied their association with β-catenin and showed that increased β-catenin expression and its nuclear translocation are associated with uPAR overexpression. Moreover, quercetin, a known inhibitor of WNT signaling (40), suppressed uPAR and uPAR-mediated increase in WNT signaling molecules. Furthermore, uPAR knockdown (pU) suppressed IR-induced WNT/β-catenin signaling both *in vitro* and *in vivo*. Taken together, this study provides direct evidence that mutual regulation mechanisms exist among uPAR and β-catenin signaling and signals underlying different processes regulating cancer cell, stemness, and adaptation to radiation treatment (Fig. 7). Recent studies have also shown that down-regulation of uPAR results in suppression of a number of β-catenin downstream targets that were identified by a two-dimensional gel electro-

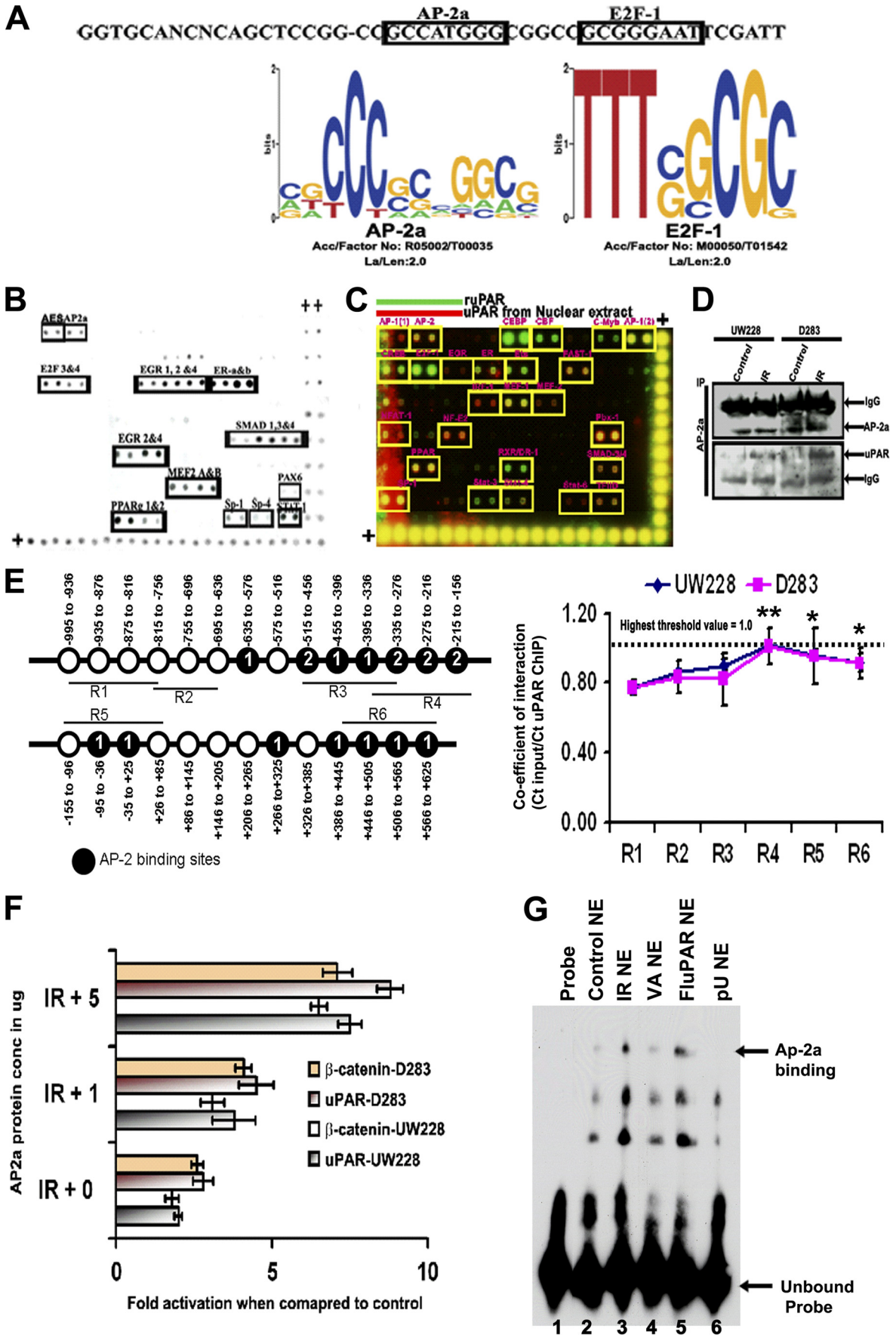
A
AP-2a
E2F-1
GGTGCANCNCAGCTCCGG-CCGCCATGGGCGGCCGCGGGAATTCGATT
AP-2a
Acc/Factor No: R05002/T00035
La/Len:2.0
E2F-1
Acc/Factor No: M00050/T01542
La/Len:2.0
B
AES/AP2a
E2F 3&4
EGR 1, 2 &4
ER-a&b
SMAD 1,3&4
EGR 2&4
MEF2 A&B
PAX6
PPARg 1&2
Sp-1
Sp-4
STAT 1
C
ruPAR
uPAR from Nuclear extract
D
UW228
D283
Control
IR
IP
AP-2a
IgG
AP-2a
uPAR
IgG
E
-995 to -936
-935 to -876
-875 to -816
-815 to -756
-755 to -696
-695 to -636
-635 to -576
-575 to -516
-515 to -456
-455 to -396
-395 to -336
-335 to -276
-275 to -216
-215 to -156
R1
R2
R3
R4
R5
R6
-155 to -96
-95 to -36
-35 to +25
+26 to +85
+86 to +145
+146 to +205
+206 to +265
+266 to+325
+326 to+385
+386 to +445
+446 to +505
+506 to +565
+566 to +625
AP-2 binding sites
UW228
D283
Highest threshold value = 1.0
Co-efficient of interaction
(Ct input/Ct uPAR ChIP)
1.20
0.80
0.40
0.00
R1
R2
R3
R4
R5
R6
F
AP2a protein conc in ug
IR + 5
IR + 1
IR + 0
β-catenin-D283
uPAR-D283
β-catenin-UW228
uPAR-UW228
0
5
10
Fold activation when comapred to control
G
Probe
Control NE
IR NE
VA NE
FluPAR NE
pU NE
Ap-2a
binding
Unbound
Probe
1 2 3 4 5 6

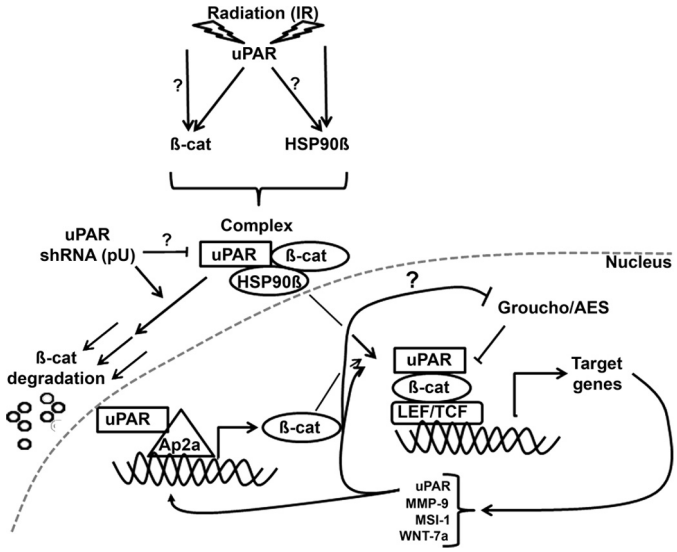

FIGURE 7. **Schematic view of mutual regulation of uPAR and β-catenin signaling as a function of IR treatment.** The IR treatment induces uPAR expression and activates uPAR-dependent cell signaling. Furthermore, IR has been shown to induce radioresistance by aberrant activation of key stem cell pathways such as WNT/β-catenin signaling. The IR-induced activation of uPAR and WNT/β-catenin signaling is mediated by increased stabilization of oncoproteins uPAR and β-catenin by forming a complex with HSP90β protein. As a result, both uPAR and β-catenin are translocated to the nucleus. In contrast, treatment with shRNA specific for uPAR (pU) showed increased β-catenin phosphorylation and degradation, thus resulting in suppression of β-catenin·TCF/LEF-mediated transactivation. When present in the nucleus, both uPAR and β-catenin were shown to mutually regulate each other's transcription. The transcription of WNT target genes via TCF/LEF transcription factors is blocked by binding of the repressor protein Groucho/AES. During active WNT signaling, β-catenin enters the nucleus and displaces Groucho from TCF/LEF and allows active complex formation for transcription of WNT target genes. From our results, we observed that uPAR can also associate with repressor protein Groucho/AES, and it is speculated that the role of uPAR in the nucleus could displace Groucho from TCF/LEF, or it is possible that the excess of uPAR is captured by the repressor protein Groucho/AES.

phoresis (41). Thus, β-catenin, which is at the crossroads of several signaling pathways, appears to be associated with uPAR-mediated signaling. Our studies have shown for first time that uPAR is associated with β-catenin, and this association is enhanced with IR treatment and furthermore that IR-treated medulloblastoma cells and CSCs showed increased nuclear association of these molecules. Although uPAR has been implicated to exist in the nucleus, the functional role of uPAR in the nucleus is not clear.

Furthermore, the role of uPAR in angiogenesis, inflammation, wound repair, and tumor progression/metastasis (42–45) is due to its ability to engage in multiple protein/protein interactions (46–50). Because uPAR is devoid of a transmembrane and cytoplasmic domain, we anticipated that association of uPAR with β-catenin would involve other interlinking molecules. To determine these associated molecules, we immunoprecipitated membrane-associated uPAR extracts and subjected them to mass spectrometry. We identified HSP90β as the prominent interacting molecule by mass spectrometry. HSP90 overexpression is known to contribute to tumor cell survival by stabilizing aberrant signaling proteins (51), including more than 100 TF and is responsible for retrograde movement of protein complexes toward the nucleus (51, 52). In adult T-cell leukemia/lymphoma cells, HSP90 inhibition retarded nuclear translocation of β-catenin (34) and indicated a possible interaction between HSP90 and β-catenin. Our subsequent immunoprecipitation results indicated that HSP90β was interlinked with both uPAR and β-catenin proteins, and together they formed a more stable uPAR·β-catenin·HSP90β complex upon IR treatment when compared with control cells. Furthermore, the inhibitors of HSP90 and WNT signaling are suggested to have promising anticancer activity in cancer stem cells (53). Interestingly, pU treatment suppressed HSP90β levels and down-regulated the WNT-β-catenin·TCF/LEF-mediated signaling.

Until now uPAR has been studied as an invasion-, migration-, and metastasis-promoting protein in existing cancers; however, the function of uPAR as a promoter of stemness was recently demonstrated in breast cancer by Jo *et al.* (11). Our studies show that uPAR interacts with AP2a (activating enhancer binding protein 2α) and E2F-1 (E2F transcription factor) proteins and their respective consensus sequence from ChIP, TF protein array, and protein·DNA array analysis. When ruPAR was used to study protein/protein interaction with known TFs, we also observed that uPAR bound specifically to CCAAT/enhancer-binding protein, core-binding factor, E2F-1, and RXR/D-1 (retinoid X receptor/down-regulator of transcription 1); conversely, when uPAR was immunoprecipi-

FIGURE 6. **uPAR associates with various TF involved in cancer progression and stemness.** *A,* ChIP uPAR was performed in UW228 and D283 control and IR-treated cells. The ChIP-eluted chromatin was subjected for cloning, sequencing, and TF binding prediction analysis as described under "Experimental Procedures." *B,* human recombinant uPAR (ruPAR) was used as bait to immunoprobe various TF using TranSignal™ TF protein arrays version I, II, and IV (MA3501, MA3502, and MA3504) with multiple TFs immobilized on the membranes. *C,* interaction of ruPAR and uPAR, immunoprecipitated from NE of IR-treated D283 cells, with different TF-binding oligonucleotide probes was studied using the protein·DNA array version I (MA1210) as described under "Experimental Procedures." Binding of uPAR to TFs was observed as spots on the x-ray film and are represented as *red* (immunoprecipitated uPAR from the NE) and *green* (ruPAR) overlapping spots in the picture. + spots shows the positive control. *D,* immunoprecipitation was done using anti-uPAR antibody, and the eluate was immunoprobed using anti-uPAR and anti-AP2a antibody. *E,* analysis of 1.6-kb 5′-flanking region consisting of the noncoding exon 1, and the first 495 bp of intron 1 of the human β-catenin gene (EMBL accession number X89448) identified 16 putative AP2a consensus sites (32). Quantitative PCR amplicons covering R1, R2, R3, R4, R5, and R6 are indicated by *black lines* below. To investigate whether uPAR binding to the β-catenin promoter is localized around these sites, we used UW228 and D283 ChIP DNA immunoprecipitated by anti-uPAR and anti-IgG antibody. Immunoprecipitated DNA was analyzed by semi-quantitative RT-PCR using ChIP-specific primers covering β-catenin promoter regions R1–R6 (primers are listed in supplemental Table 4). The coefficient of uPAR interaction with different regions (R1–R6) in the β-catenin promoter was quantified (*Ct* value of input DNA/*Ct* value of uPAR ChIP DNA) and represented graphically. The uPAR enrichment at R4 (coefficient of interaction = 1.0), which includes six putative AP2-binding sites, was greater than at other regions containing AP2 (R3, R5, and R6) or no AP2 (R1 and R2). The negative control anti-IgG ChIP DNA did not show any amplification with R1–R6 primers. ($n = 3$; *, $p < 0.05$; **, $p < 0.01$). *F,* transcript levels of uPAR, β-catenin were analyzed in the Ap-2a (0, 1, and 5 μg/ml) in combination with IR-treated UW228 and D283 cells and represented graphically as the fold change expression compared with the control cells. A sequence of the GAPDH gene, not regulated by AP-2, was used as the internal control. The *bar graphs* are means ± S.D. from three independent experiments ($p < 0.01$). *G,* EMSA was performed with 2 μg of NE from treated cells. *Lane 1* is for the AP-2(1) probe in the absence of NE; *lanes 2* and *3* show NE of control and IR-treated D283 cells, respectively; and *lanes 4–6* show NE of D283 cells treated with vector alone (*VA*), Fl-uPAR, and pU plasmids, respectively.

tated from nuclear extracts, only a few TFs showed unique interaction, which was not seen when ruPAR alone was used, probably indicating that whole molecule uPAR is capable of interactions that are modulated by other nuclear factors. Interestingly, interaction with AP2, AP1 (activator protein 1), FAST-1 (forkhead activin signal transducer-1), MEF-1 (myocyte-specific enhancer factor 1), Pbx-1 (pre-B-cell leukemia homeobox 1), and peroxisome proliferator-activated receptors was observed when both ruPAR and nuclear uPAR were used.

It is interesting to note that the promoter region of uPAR possesses Sp1 (specificity protein 1), AP1, AP2, and NF-κB (nuclear factor-κB) TF-binding sites (54). The presence of AP1 and AP2 in the uPAR promoter region and the ability of uPAR to interact with these TFs probably indicate that uPAR is capable of self-regulation to a large extent and is capable of regulating other molecules as well. In our previous studies, we observed such a regulation and demonstrated that suppression of uPAR alone caused suppression of uPA expression (55) It is also interesting to note that AP-1-binding sites are present on the WNT promoter (56, 57), thus indicating that both WNT and uPAR probably regulate expression of each other to a certain extent, and overexpression of uPAR would cause activation of WNT signaling as observed in our results. Previous studies have also shown that the β-catenin promoter possesses a number of high affinity TF-binding sites, including AP2, SP1, NF-κB, and EGR1 (32), suggesting that uPAR can also regulate β-catenin, which was also seen in our results. From our studies of uPAR ChIP, TF protein, and protein·DNA array, we confirmed that uPAR associates with transcription factor AP2a and enhances β-catenin gene transcription. Furthermore, we also observed that uPAR overexpression promotes AP2 activity, which could be one of the mechanisms of increased β-catenin expression. The presence of AP1 and AP2 binding regions seen in the promoters of various molecules need not indicate that all may be regulated by uPAR. However, it is indeed interesting to note that overexpression of uPAR was sufficient to up-regulate some of them, including β-catenin. Studies indicate that uPAR is not required for development or fertility in mice (58) probably indicating that uPAR may have an acquired role in cancer stem cell maintenance. Taken together, our data show that uPAR overexpression up-regulated WNT-β-catenin signaling by stabilization of β-catenin protein via HSP90 association, increased transcription of the β-catenin gene, and increased transcription of WNT ligand genes such as WNT-7a. All these mechanisms contribute to increased accumulation of nuclear β-catenin and consequently to activation of the WNT target gene transcription. As a result, targeting uPAR in cancer patients showing the presence of cancer stem cells undergoing radiotherapy will have favorable therapeutic implications.

Acknowledgments—We thank Peggy Mankin and Noorjehan Ali for their technical assistance, Shellee Abraham for manuscript preparation, and Diana Meister and Sushma Jasti for manuscript review. We thank Dr. Ali-Osman, Duke University Medical Center, for providing UW228 cells.

REFERENCES

1. Lannering, B., Sandström, P. E., Holm, S., Lundgren, J., Pfeifer, S., Samuelsson, U., Strömberg, B., Gustafsson, G., and Swedish Childhood CNS Tumor Working Group (VCTB) (2009) Classification, incidence, and survival analyses of children with CNS tumors diagnosed in Sweden 1984–2005. *Acta Paediatr.* **98,** 1620–1627
2. Dhall, G. (2009) Medulloblastoma. *J. Child Neurol.* **24,** 1418–1430
3. Romer, J., Nielsen, B. S., and Ploug, M. (2004) The urokinase receptor as a potential target in cancer therapy. *Curr. Pharm. Des.* **10,** 2359–2376
4. Sidenius, N., and Blasi, F. (2003) The urokinase plasminogen activator system in cancer. Recent advances and implication for prognosis and therapy. *Cancer Metastasis Rev.* **22,** 205–222
5. de Witte, J. H., Foekens, J. A., Brünner, N., Heuvel, J. J., van Tienoven, T., Look, M. P., Klijn, J. G., Geurts-Moespot, A., Grebenchtchikov, N., Benraad, T., and Sweep, C. G. (2001) Prognostic impact of urokinase-type plasminogen activator receptor (uPAR) in cytosols and pellet extracts derived from primary breast tumors. *Br. J. Cancer* **85,** 85–92
6. Gorantla, B., Asuthkar, S., Rao, J. S., Patel, J., and Gondi, C. S. (2011) Suppression of the uPAR-uPA system retards angiogenesis, invasion, and *in vivo* tumor development in pancreatic cancer cells. *Mol. Cancer Res.* **9,** 377–389
7. Killeen, S., Hennessey, A., El Hassan, Y., and Waldron, B. (2008) The urokinase plasminogen activator system in cancer. A putative therapeutic target? *Drug News Perspect.* **21,** 107–116
8. D'Alessio, S., Margheri, F., Pucci, M., Del Rosso, A., Monia, B. P., Bologna, M., Leonetti, C., Scarsella, M., Zupi, G., Fibbi, G., and Del Rosso, M. (2004) Antisense oligodeoxynucleotides for urokinase-plasminogen activator receptor have anti-invasive and anti-proliferative effects *in vitro* and inhibit spontaneous metastases of human melanoma in mice. *Int. J. Cancer* **110,** 125–133
9. Lin, L., Gårdsvoll, H., Huai, Q., Huang, M., and Ploug, M. (2010) Structure-based engineering of species selectivity in the interaction between urokinase and its receptor. Implication for preclinical cancer therapy. *J. Biol. Chem.* **285,** 10982–10992
10. Nalla, A. K., Asuthkar, S., Bhoopathi, P., Gujrati, M., Dinh, D. H., and Rao, J. S. (2010) Suppression of uPAR retards radiation-induced invasion and migration mediated by integrin β1/FAK signaling in medulloblastoma. *PLoS One* **5,** e13006
11. Jo, M., Eastman, B. M., Webb, D. L., Stoletov, K., Klemke, R., and Gonias, S. L. (2010) Cell signaling by urokinase-type plasminogen activator receptor induces stem cell-like properties in breast cancer cells. *Cancer Res.* **70,** 8948–8958
12. Fan, X., and Eberhart, C. G. (2008) Medulloblastoma stem cells. *J. Clin. Oncol.* **26,** 2821–2827
13. Pomeroy, S. L., Tamayo, P., Gaasenbeek, M., Sturla, L. M., Angelo, M., McLaughlin, M. E., Kim, J. Y., Goumnerova, L. C., Black, P. M., Lau, C., Allen, J. C., Zagzag, D., Olson, J. M., Curran, T., Wetmore, C., Biegel, J. A., Poggio, T., Mukherjee, S., Rifkin, R., Califano, A., Stolovitzky, G., Louis, D. N., Mesirov, J. P., Lander, E. S., and Golub, T. R. (2002) Prediction of central nervous system embryonal tumoroutcome based on gene expression. *Nature* **415,** 436–442
14. Ellison, D. W., Onilude, O. E., Lindsey, J. C., Lusher, M. E., Weston, C. L., Taylor, R. E., Pearson, A. D., and Clifford, S. C. (2005) β-Catenin status predicts a favorable outcome in childhood medulloblastoma. The United Kingdom Children's Cancer Study Group Brain Tumor Committee. *J. Clin. Oncol.* **23,** 7951–7957
15. Logan, C. Y., and Nusse, R. (2004) The WNT signaling pathway in development and disease. *Annu. Rev. Cell Dev. Biol.* **20,** 781–810
16. Mann, B., Gelos, M., Siedow, A., Hanski, M. L., Gratchev, A., Ilyas, M., Bodmer, W. F., Moyer, M. P., Riecken, E. O., Buhr, H. J., and Hanski, C. (1999) Target genes of β-catenin-T cell-factor/lymphoid-enhancer-factor signaling in human colorectal carcinomas. *Proc. Natl. Acad. Sci. U.S.A.* **96,** 1603–1608
17. Jankun, J., Merrick, H. W., and Goldblatt, P. J. (1993) Expression and localization of elements of the plasminogen activation system in benign breast disease and breast cancers. *J. Cell. Biochem.* **53,** 135–144
18. Dumler, I., Stepanova, V., Jerke, U., Mayboroda, O. A., Vogel, F., Bouvet, P., Tkachuk, V., Haller, H., and Gulba, D. C. (1999) Urokinase-induced

mitogenesis is mediated by casein kinase 2 and nucleolin. *Curr. Biol.* **9,** 1468–1476
19. Asuthkar, S., Nalla, A. K., Gondi, C. S., Dinh, D. H., Gujrati, M., Mohanam, S., and Rao, J. S. (2011) Gadd45a sensitizes medulloblastoma cells to irradiation and suppresses MMP-9-mediated EMT. *Neuro-oncol.* **13,** 1059–1073
20. Velpula, K. K., Dasari, V. R., Tsung, A. J., Dinh, D. H., and Rao, J. S. (2011) Cord blood stem cells revert glioma stem cell EMT by down regulating transcriptional activation of Sox2 and Twist1. *Oncotarget* 2, 1028–1042
21. Thomas, S., Chiriva-Internati, M., and Shah, G. V. (2007) Calcitonin receptor-stimulated migration of prostate cancer cells is mediated by urokinase receptor-integrin signaling. *Clin. Exp. Metastasis* **24,** 363–377
22. Lakka, S. S., Gondi, C. S., Dinh, D. H., Olivero, W. C., Gujrati, M., Rao, V. H., Sioka, C., and Rao, J. S. (2005) Specific interference of urokinase-type plasminogen activator receptor and matrix metalloproteinase-9 gene expression induced by double-stranded RNA results in decreased invasion, tumor growth, and angiogenesis in gliomas. *J. Biol. Chem.* **280,** 21882–21892
23. Nesvizhskii, A. I., Keller, A., Kolker, E., and Aebersold, R. (2003) A statistical model for identifying proteins by tandem mass spectrometry. *Anal. Chem.* **75,** 4646–4658
24. Lakka, S. S., Rajan, M., Gondi, C., Yanamandra, N., Chandrasekar, N., Jasti, S. L., Adachi, Y., Siddique, K., Gujrati, M., Olivero, W., Dinh, D. H., Kouraklis, G., Kyritsis, A. P., and Rao, J. S. (2002) Adenovirus-mediated expression of antisense MMP-9 in glioma cells inhibits tumor growth and invasion. *Oncogene* **21,** 8011–8019
25. Rich, J. N. (2007) Cancer stem cells in radiation resistance. *Cancer Res.* **67,** 8980–8984
26. Dierick, H., and Bejsovec, A. (1999) Cellular mechanisms of wingless/WNT signal transduction. *Curr. Top. Dev. Biol.* **43,** 153–190
27. Rezza, A., Skah, S., Roche, C., Nadjar, J., Samarut, J., and Plateroti, M. (2010) The overexpression of the putative gut stem cell marker Musashi-1 induces tumorigenesis through WNT and Notch activation. *J. Cell Sci.* **123,** 3256–3265
28. Behzadian, M. A., Windsor, L. J., Ghaly, N., Liou, G., Tsai, N. T., and Caldwell, R. B. (2003) VEGF-induced paracellular permeability in cultured endothelial cells involves urokinase and its receptor. *FASEB J.* **17,** 752–754
29. Wong, N. A., and Pignatelli, M. (2002) β-Catenin. A linchpin in colorectal carcinogenesis? *Am. J. Pathol.* **160,** 389–401
30. Ingraham, C. A., Park, G. C., Makarenkova, H. P., and Crossin, K. L. (2011) Matrix metalloproteinase (MMP)-9 induced by WNT signaling increases the proliferation and migration of embryonic neural stem cells at low O_2 levels. *J. Biol. Chem.* **286,** 17649–17657
31. Ragno, P. (2006) The urokinase receptor. A ligand or a receptor? Story of a sociable molecule. *Cell. Mol. Life Sci.* **63,** 1028–1037
32. Nollet, F., Berx, G., Molemans, F., and van Roy, F. (1996) Genomic organization of the human β-catenin gene (CTNNB1). *Genomics* **32,** 413–424
33. de Crozé N., Maczkowiak, F., and Monsoro-Burq, A. H. (2011) Reiterative AP2a activity controls sequential steps in the neural crest gene regulatory network. *Proc. Natl. Acad. Sci. U.S.A.* **108,** 155–160
34. Kurashina, R., Ohyashiki, J. H., Kobayashi, C., Hamamura, R., Zhang, Y., Hirano, T., and Ohyashiki, K. (2009) Anti-proliferative activity of heat shock protein (Hsp) 90 inhibitors via β-catenin/TCF7L2 pathway in adult T cell leukemia cells. *Cancer Lett.* **284,** 62–70
35. Xiang, Y., Qin, X. Q., Liu, H. J., Tan, Y. R., Liu, C., and Liu, C. X. (2012) Identification of transcription factors regulating CTNNAL1 expression in human bronchial epithelial cells. *PLoS One* **7,** e31158
36. Decary, S., Decesse, J. T., Ogryzko, V., Reed, J. C., Naguibneva, I., Harel-Bellan, A., and Cremisi, C. E. (2002) The retinoblastoma protein binds the promoter of the survival gene *bcl-2* and regulates its transcription in epithelial cells through transcription factor AP-2. *Mol. Cell. Biol.* **22,** 7877–7888
37. Louis, D. N., Ohgaki, H., Wiestler, O. D., Cavenee, W. K., Burger, P. C., Jouvet, A., Scheithauer, B. W., and Kleihues, P. (2007) The 2007 WHO classification of tumors of the central nervous system. *Acta Neuropathol.* **114,** 97–109
38. Eberhart, C. G., Tihan, T., and Burger, P. C. (2000) Nuclear localization and mutation of β-catenin in medulloblastomas. *J. Neuropathol. Exp. Neurol.* **59,** 333–337
39. Wu, B., Crampton, S. P., and Hughes, C. C. (2007) WNT signaling induces matrix metalloproteinase expression and regulates T cell transmigration. *Immunity* **26,** 227–239
40. Park, C. H., Chang, J. Y., Hahm, E. R., Park, S., Kim, H. K., and Yang, C. H. (2005) Quercetin, a potent inhibitor against β-catenin/TCF signaling in SW480 colon cancer cells. *Biochem. Biophys. Res. Commun.* **328,** 227–234
41. Saldanha, R. G., Xu, N., Molloy, M. P., Veal, D. A., and Baker, M. S. (2008) Differential proteome expression associated with urokinase plasminogen activator receptor (uPAR) suppression in malignant epithelial cancer. *J. Proteome Res.* **7,** 4792–4806
42. Blasi, F., and Carmeliet, P. (2002) uPAR. A versatile signaling orchestrator. *Nat. Rev. Mol. Cell Biol.* **3,** 932–943
43. Del Rosso, M. (2011) uPAR in angiogenesis regulation. *Blood* **117,** 3941–3943
44. Jo, M., Takimoto, S., Montel, V., and Gonias, S. L. (2009) The urokinase receptor promotes cancer metastasis independently of urokinase-type plasminogen activator in mice. *Am. J. Pathol.* **175,** 190–200
45. Rao, J. S., Gondi, C., Chetty, C., Chittivelu, S., Joseph, P. A., and Lakka, S. S. (2005) Inhibition of invasion, angiogenesis, tumor growth, and metastasis by adenovirus-mediated transfer of antisense uPAR and MMP-9 in non-small cell lung cancer cells. *Mol. Cancer Ther.* **4,** 1399–1408
46. Koshelnick, Y., Ehart, M., Hufnagl, P., Heinrich, P. C., and Binder, B. R. (1997) Urokinase receptor is associated with the components of the JAK1/STAT1 signaling pathway and leads to activation of this pathway upon receptor clustering in the human kidney epithelial tumor cell line TCL-598. *J. Biol. Chem.* **272,** 28563–28567
47. Liu, D., Aguirre Ghiso, J., Estrada, Y., and Ossowski, L. (2002) EGFR is a transducer of the urokinase receptor-initiated signal that is required for *in vivo* growth of a human carcinoma. *Cancer Cell* **1,** 445–457
48. Mekkawy, A. H., De Bock, C. E., Lin, Z., Morris, D. L., Wang, Y., and Pourgholami, M. H. (2010) Novel protein interactors of urokinase-type plasminogen activator receptor. *Biochem. Biophys. Res. Commun.* **399,** 738–743
49. Preissner, K. T., Kanse, S. M., and May, A. E. (2000) Urokinase receptor. A molecular organizer in cellular communication. *Curr. Opin. Cell Biol.* **12,** 621–628
50. Resnati, M., Pallavicini, I., Wang, J. M., Oppenheim, J., Serhan, C. N., Romano, M., and Blasi, F. (2002) The fibrinolytic receptor for urokinase activates the G protein-coupled chemotactic receptor FPRL1/LXA4R. *Proc. Natl. Acad. Sci. U.S.A.* **99,** 1359–1364
51. Pratt, W. B., Galigniana, M. D., Harrell, J. M., and DeFranco, D. B. (2004) Role of hsp90 and the hsp90-binding immunophilins in signaling protein movement. *Cell. Signal.* **16,** 857–872
52. Pratt, W. B., and Toft, D. O. (2003) Regulation of signaling protein function and trafficking by the hsp90/hsp70-based chaperone machinery. *Exp. Biol. Med.* **228,** 111–133
53. Ruden, D. M., Xiao, L., Garfinkel, M. D., and Lu, X. (2005) Hsp90 and environmental impacts on epigenetic states. A model for the trans-generational effects of diethylstilbestrol on uterine development and cancer. *Hum. Mol. Genet.* **14,** R149–R155
54. Wang, Y. (2001) The role and regulation of urokinase-type plasminogen activator receptor gene expression in cancer invasion and metastasis. *Med. Res. Rev.* **21,** 146–170
55. Gondi, C. S., Lakka, S. S., Yanamandra, N., Siddique, K., Dinh, D. H., Olivero, W. C., Gujrati, M., and Rao, J. S. (2003) Expression of antisense uPAR and antisense uPA from a bicistronic adenoviral construct inhibits glioma cell invasion, tumor growth, and angiogenesis. *Oncogene* **22,** 5967–5975
56. Katoh, M., and Katoh, M. (2007) AP1- and NF-κB-binding sites conserved among mammalian WNT10B orthologs elucidate the TNFα-WNT10B signaling loop implicated in carcinogenesis and adipogenesis. *Int. J. Mol. Med.* **19,** 699–703
57. Le Floch, N., Rivat, C., De Wever, O., Bruyneel, E., Mareel, M., Dale, T., and Gespach, C. (2005) The proinvasive activity of WNT-2 is mediated through a noncanonical WNT pathway coupled to GSK-3β and c-Jun/AP-1 signaling. *FASEB J.* **19,** 144–146
58. Bugge, T. H., Suh, T. T., Flick, M. J., Daugherty, C. C., Rømer, J., Solberg, H., Ellis, V., Danø, K., and Degen, J. L. (1995) The receptor for urokinase-type plasminogen activator is not essential for mouse development or fertility. *J. Biol. Chem.* **270,** 16886–16894